Supplemental Material

Electrostatically induced phononic crystal

D. Hatanaka,[1,*] A. Bachtold,[2] and H. Yamaguchi[1]

[1] *NTT Basic Research Laboratories, NTT Corporation, Atsugi-shi, Kanagawa 243-0198, Japan*

[2] *ICFO-Institut de Ciencies Fotoniques, The Barcelona Institute of Science and Technology, Castelldefels (Barcelona) 08860, Spain*

1 Comparison between unit structures with and without SiO_2 supports

We compare the effect of unit structures with and without SiO_2 support substrate on simulation results. Figures S1(a) shows a schematic of the structure with/without the support (right/left). The design containing the substrate is fixed at the bottom of the substrates and one without it is fixed at both clamping edges of the graphene. The former is adopted to introduce perfect matched layers (PMLs) to the outer substrate domains. Floquet boundary condition (BC) is applied in both structures. Figure S1(b) shows the maximum static displacement and edge stress in the device as function of V_g ranging from 0 V to 5V calculated from the structure with (blue) and without the support (red). To confirm the availability of the support, we also calculate the dispersion relation at $V_g = 6$ V in these unit cells as shown in Fig. S1(c). Although the bands shift up to high frequency due to the existence of the support (blue) compared to without one (red) in spectral range > 30 MHz, they are in good agreement each other in the spectral range < 30 MHz, where bandgaps and band flattening occur. Thus, these results obtained from two configurations indicate that the FEM analysis can be approximated, particularly around the bandgap spectral regions, by just considering a suspended graphene sheet.

2 Comparison between electromechanical and pure mechanical approaches in FEM calculations

Two possible approaches in FEM calculation are used in the manuscript to simulate the graphene WG. One is an electromechanical approach which simulates electrostatic fields and the resultant mechanical dynamics of an elastic continuum by using electrical input such as voltage. This enables calculation of mutual interactions between electrostatic and mechanical fields, thus offering detail results on the mechanical properties of the device. A change in electric field due to the mechanical deformation can be taken into the calculation, and for instance, electrostatic softening can be reproduced. This approach is mainly used in the calculations in the manuscript. The other is pure mechanical approach which only calculates the mechanical dynamics of the device. Since the electrostatic pressure is given as equation (1) in the manuscript, the dynamics of deformation and vibration of the graphene can be approximately estimated from the case where the electrostatic pressure is used as input to be directly applied to the graphene. As a result, this approach saves the computational cost and is useful when calculating a large-scale structure such as the transmission characteristics of the graphene WG as shown in Fig. 5(b) in the manuscript. Although this sometime makes the deviation from the response of a real device, the calculation results can reproduce it very well in low frequency regime where bandgaps appear, and low gate voltages V_gs where capacitance variation caused by displacement of the graphene is negligibly small.

Figure S2(a) shows the static displacement of the unit structure with $d = 85$ nm as shown in the left of Fig. S1(a), which is induced by the electrostatic force with the electromechanical (red) and pure mechanical (blue) approaches. The calculated results are good agreement each other except $V_g > 3$ V where an increase in the capacitance due to reduction in the graphene-electrode separation becomes effective in the resultant electrostatic force exerted on the graphene. Figure S2(b) reveals the dispersion relation of the graphene WG with $d = 130$ nm at $V_g = 4$ V calculated from the electromechanical (red) and pure mechanical (blue)

approaches. In both cases, first and second bandgaps appear below 20 MHz, whereas small frequency deviations between them can be found where the bands by the mechanical approach are lower than those by the electromechanical one, and the deviation is being increased with increasing frequency. Thus, the pure mechanical approach is an efficient method to simulate the frequency response of the device in low spectral range (< 20 MHz) at moderate V_{g}s.

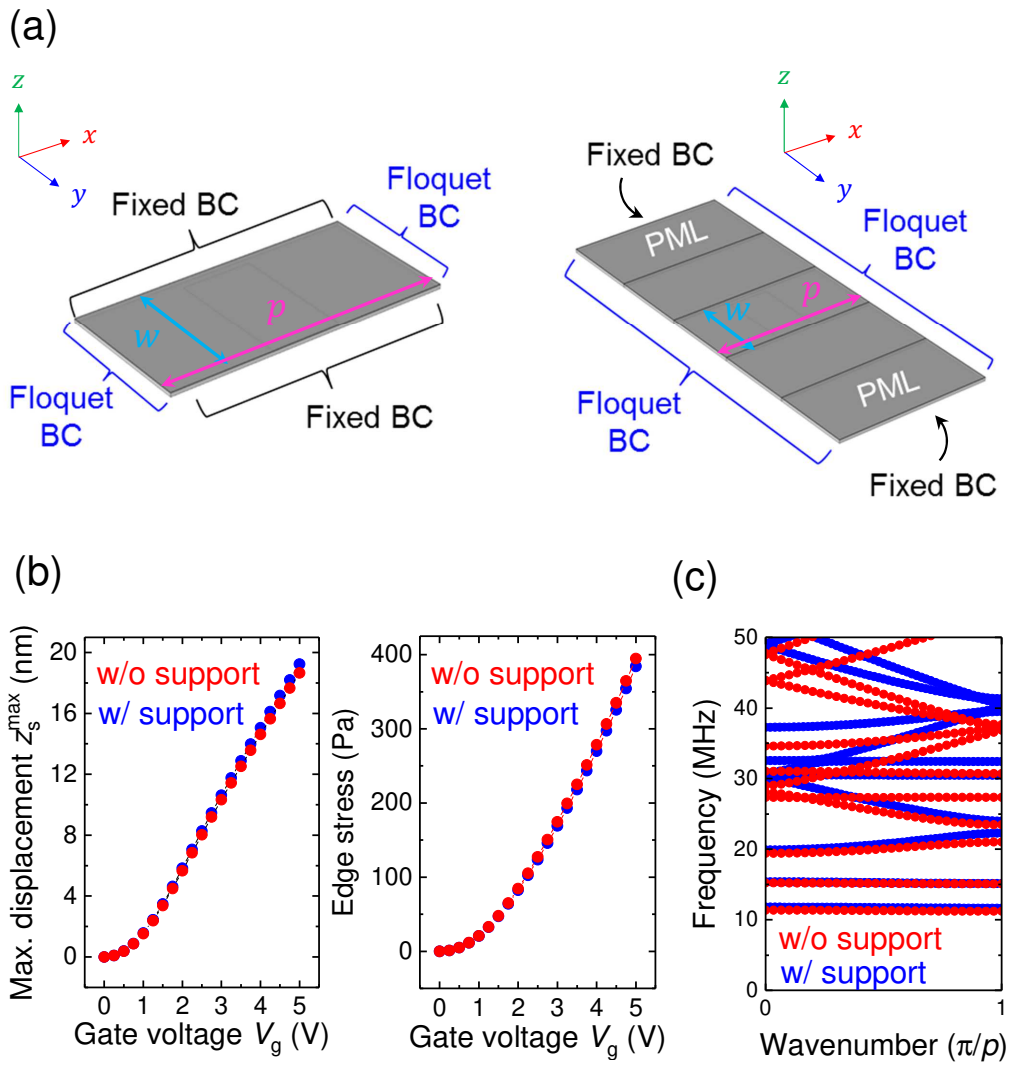

Figure S1: **The effect of a model with and without a substrate in FEM calculations.** (**a**) The unit cell with (right) and without supports (left) with $p = 2a$ is shown. The left schematic and the center domain of the right schematic indicate the suspended graphene WG part, and both side-domains of the right one contain the supporting substrates. The suspended graphene part is composed of vacuum, graphene and vacuum layers from the top, and the support parts consist of vacuum, graphene and SiO_2 layers. PMLs are introduced in both out-side domains of the unit cell as shown in the right schematic. The suspended graphene edges at $x = \pm p/2$ are given Floquet BC. The graphene edges $y = \pm w/2$ in the left cell and the bottom of the SiO_2 supports in the right one are given fixed BC. (**b**) The static displacement at $(x, y) = (0, 0)$ and the stress at $(x, y) = (0, \pm w/2)$ calculated from the unit cell with (blue) and without the support (red) are shown in the left and right panels respectively. (**c**) The dispersion relations from the cell with (blue) and without the support (red) are shown.

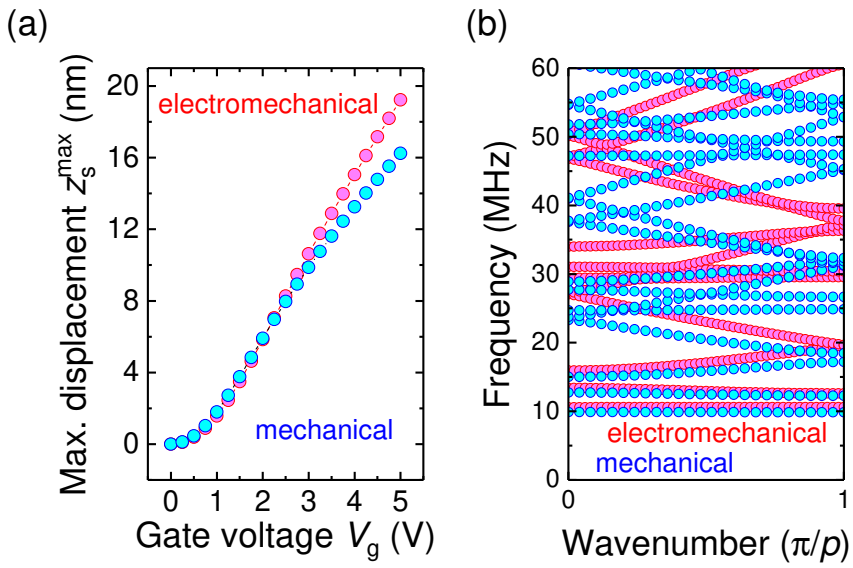

Figure S2: **FEM calculation from different approaches.** (**a**) The static displacement at $(x, y) = (0, 0)$ of the device with $d = 85$ nm and $p = 2a$ as function of gate voltage V_g calculated from the electromechanical (red) and pure mechanical (blue) approaches. (**b**) The dispersion relation of the device with $d = 130$ nm and at $V_g = 4$ V calculated from the electromechanical (red) and pure mechanical (blue) approaches.